Results in Engineering 25 (2025) 104329

Contents lists available at ScienceDirect

Results in Engineering

journal homepage: www.sciencedirect.com/journal/results-in-engineering

Research paper

Adaptive landslide monitoring in wireless sensor networks using FLPSO-based MIP systems

Lingaraj K [a], Rashmi Laxmikant Malghan [b,*], KarthiK Rao M C [c,*], Lalit Garg [d]

[a] Department of Computer Science and Engineering, Rao Bahadur Y Mahabaleswarappa Engineering College, Cantonment, Ballari, 583104, Karnataka, India
[b] Department of Data Science and Computer Applications, Manipal Institute of Technology, Manipal Academy of Higher Education, Manipal, 576104, Karnataka, India
[c] Department of Mechatronics Engineering, Manipal Institute of Technology, Manipal Academy of Higher Education, Manipal, 576104, Karnataka, India
[d] Department of Computer Information System (CIS), Faculty of Information Communication Technology (ICT), University of Malta, Msidal, 2080, Malta

ARTICLE INFO

Keywords:
WSN
Landslide
Source node
Stress
Monitoring system
Fuzzy logic

ABSTRACT

Landslides are one of the most significant natural geological hazards, capable of causing extensive damage to lives, infrastructure, and property. These events are often triggered by specific geological and environmental conditions that can be monitored utilizing advanced technologies such as Wireless Sensor Networks (WSNs). This study introduces a novel itinerary planning approach for WSNs, employing the Fuzzy Logic-based Particle Swarm Optimization (FLPSO) technique, which integrates Fuzzy Logic and Particle Swarm Optimization methodologies. The primary objective of this approach is to minimize the energy consumption in large-scale WSNs, thereby enhancing their efficiency for landslide detection systems. The proposed method improves on traditional network grouping methods by optimizing energy usage across sensor nodes. A case study was conducted in Shiradi village, Mangalore, India, an area characterized by high annual rainfall and changing climatic patterns. Over a year, data was collected and analyzed to evaluate the system's potential for accurate landslide hazard predictions. The soil suction stress was calculated using laboratory tests, incorporating various geotechnical and unsaturated soil parameters specific to the study area. The experimental results demonstrated that energy-efficient nodes not only have a longer operational lifespan and greater adaptability to environmental changes, but also exhibit superior performance compared to current methods, with improvements of 14.15% in Packet Delivery Ratio (PDR), 11.15% in Energy Delay Product (EDP), 10.15% in Packet Loss Ratio (PLR), 22.1% in task delay, and 20.1% in throughput.

1. Introduction

Landslides are one of the most significant natural geological hazards, posing serious threats to human life, infrastructure, and property. These phenomena are often triggered by complex interactions between geological, hydrological, and environmental factors, making their prediction and monitoring a challenging task [1–3]. Heavy rain, in particular, plays a critical role in destabilizing slopes, leading to soil movement and eventual failure. As rainfall patterns become increasingly unpredictable due to climate change, the need for effective landslide monitoring systems has become more pressing.

The advent of advanced technologies, such as Wireless Sensor Networks (WSNs), has opened new avenues for real-time monitoring and early warning systems. WSNs offer the ability to monitor key variables, such as soil moisture, suction stress, and slope movement, by deploying sensor nodes in vulnerable areas [4–7]. However, these systems face significant challenges, including energy constraints, data latency, and network reliability. Optimizing these systems is critical to ensure their long-term functionality and effectiveness in disaster-prone regions.

This study introduces a novel approach to itinerary planning for WSNs using the Fuzzy Logic-based Particle Swarm Optimization (FLPSO) technique. By combining Fuzzy Logic and Particle Swarm Optimization, the proposed method addresses key limitations of traditional network grouping methods, such as high energy consumption and inefficient data routing [8]. The FLPSO algorithm is designed to improve the energy efficiency of sensor nodes, thus extending the network operational life and improving adaptability to environmental changes [9,10]. To evaluate the efficacy of the proposed method, a case study was conducted in Shiradi village, Mangalore, India, a region characterized by high annual rainfall and a history of landslides. Over a year, data was collected and analyzed to assess the system's potential for accurate landslide hazard predictions. The study highlights the significant improvements of-

* Corresponding author.
E-mail addresses: rashmi.malghan@manipal.edu (R.L. Malghan), rao.karthik@manipal.edu (K. Rao M C).

https://doi.org/10.1016/j.rineng.2025.104329
Received 31 August 2024; Received in revised form 29 January 2025; Accepted 9 February 2025

Available online 14 February 2025

fered by FLPSO over existing methods, demonstrating its effectiveness in reducing energy consumption and improving network performance [11–16]. The results of this study underscore the critical role of advanced optimization techniques in the development of robust landslide monitoring systems [17]. By leveraging the strengths of FLPSO, this research contributes to the overall goal of improving disaster preparedness and mitigating the impacts of natural hazards.

1.1. Related work

The design of optimal monitoring systems for phenomena such as landslides remains a significant challenge due to several factors. The heterogeneous nature of sensing technologies presents a substantial obstacle. These technologies exhibit considerable variation in their operational mechanisms, topological arrangements, reliability, cost, and complexity, thereby impeding the identification of a universally suitable solution. In addition, the interdisciplinary nature of the monitoring, which includes aspects of geology, engineering, and data analysis, introduces an additional layer of complexity. Despite these challenges, researchers have proposed various monitoring and prediction methods, employing diverse technologies to successfully anticipate landslides.

1.1.1. Early warning landslide monitoring system

Wireless sensor nodes that contain MEMS and IMU nodes can identify mobility in soil gradients. In [22], the researchers described a monitoring device capable of identifying a boulder drop event and the key characteristics of the safety obstacle, which may be made up of a gabion mesh or concrete blocks. The system design is configurable, with sensing components and a monitoring unit at the job site. These devices collect data on the tremors and slopes of a falling boulder safety obstacle. The information is stored on an HTTP server that manages gathering and impulsive communications in the event of condemnation. The acquired data were summarized and examined using an online interface.

Despite the capability of IMU-based WSNs to gauge surges and cycles, an enormous amount of research is required to characterize and differentiate various forms of slope mobility. Accelerometer information on the behavior of tangible objects has been shown to exhibit unique trends in numerous studies [23]. Using accelerometer and gyroscope signals to categorize motions, the authors conducted exploratory research employing pattern identification. This knowledge provides a basic understanding of landslides in civil engineering and aids in analyzing the integrity of slopes and implementing safeguard and prevention designs. In [24], researchers describe a framework comprised of WSN nodes communicating with a single central station using the 802.11 g standard [25]. A caravan with workstations for the on-site evaluation of information and wireless transmission constitutes the station. This link facilitates communication over the internet using a central database system. Studies are carried out via a pebble affixed to a sensor device and the findings are provided to illustrate the various inertial measurement unit (IMU) information related to potential mass shifts. The authors of [26] suggested a design approach for acoustic emission to reveal stress-strain circumstances within subterranean rock masses. Identifying microseismic occurrences from a vulnerable rock structure is essential to find expanding fissures and to analyze the trigger mechanisms that cause future catastrophes. The nodes that use Micro-Electro-Mechanical System (MEMS) produce output [27] and the MicaZ [28] mote are deployed at the location. Each node has a microprocessor and a 2.4 GHz receiver. Due to the logical arrangement of the equipment, the multihop propagation scheme is ideally adapted for this investigation. Efforts are being made to analyze the pipeline mode to improve efficiency and minimize data loss.

Measurements from MEMS tilt sensors were integrated into the system integrato gestione monitoraggion allerta(SIGMA) program employing a decisional method at an experiment point in Darjeeling to exceed the rainfall benchmark that is considered statistically significant. As a consequence of incorporating tilt meter readings into the SIGMA approach, the number of incorrect warnings reduced from 70 to 38, and the trustworthiness factor increased from 18.10 to 20:50 [29]. The primary issue for designers and academics in areas susceptible to landslides is the energy used by WSN networks. The main obstacles are correctly detecting activities, transferring data to the server, and conserving the power of the sensor nodes. SMARTCONE is suggested to reduce its power use in dormant circumstances by placing the CPU and nodes in a sleep state with 0.05 mA at 3.6 V. Sensor nodes are installed approximately 60 centimeters below the surface [30,31].

Setting up a WSN network for a large territory in a region prone to landslides is less expensive. An accelerometer provides a low-cost solution for obtaining displacement, inclination, and tremor data. Information is transferred via Zigbee to the bridge node and then to the data center for analysis [32].

Reference investigators [33] have implemented a WSN built on LoRa innovation in a landslide area located on an inhabitable mountainside. The objective of their study was to examine the suitability of a LoRa-based system in difficult circumstances, with an emphasis on communication zone coverage and the localization of a specific node in the system through Received Signal Strength Intensity (RSSI). However, a comprehensive explanation of the hardware design of the sensor node, its fixing processes on the sloping side, and the power-related attributes of each component is not discernible. The authors of [34] present a methodology for monitoring landslides using a LoRa system and smart sensing technology to measure the movement of the deluge and landslide in Shuicheng. The complete description of the architecture encompasses its overall structure and the development of its hardware and software components. The study presents the potential for the points to function in standard or diminished power modes, resulting in a decreased current intake of 1 mA.

The article referenced in [35] presents a LoRa-based wireless surveillance instrument that can be applied to structural health monitoring (SHM). In smart cities, remote structural health monitoring (RSHM) is an ideal tool to measure the essential harm done to urban structures. The referenced document suggests TenSense M30, an IoT sensor node that allows a wide interaction reach with prolonged power time, to track the condition of the bolt joints. TenSense M30 has an environmental impact that can be used to add value to existing buildings. Hardware and testing methods are provided.

In [36], a clustering and multi-hop protocol is presented to predict landslides. It employs a signal to transmit the clustering method to all nodes in order to choose the cluster heads (CHs) and is regularly activated to conserve assets. The information is sent to the central station (BS) by effectively balancing the number of steps against the amount of resources required for each delivery. In [37], an unsupervised landslide tracking system built around WSNs is suggested, in which smart agents constantly gather and analyze the data, including ground accelerations and the position of sensor nodes in conjunction with the gradient.

In [38], an effective WSN is suggested to assess the threat of avalanches. The information gathered by the distributed nodes is transmitted to BS via the Internet in order to track different metrics such as energy consumption, radio link, etc. Similarly, researchers in [39] suggest an energy-efficient method to gather data for rainfall-induced landslide detection systems. The objective of [39] is to decrease the amount of resources used by the nodes, which has been accomplished by using a wavelet-based sampling technique to determine the optimal processing velocity for the sensors.

Aibek Musaev [18] came up with an idea for a model tool to test and apply investigation theories and ideas on the detection of disasters. He also makes suggestions about the present method to find the sites of 137 landslides in 2014. This page also talks about a live example of a landslip detection technique and how its findings are shown on a web map. This plan is called LITMUS. It is a method for finding landslides that uses more than one utility and shows more than one danger. Radar polarimetry is employed in [19] to find and track disasters (LDCSPC). They came up with a plan to use POLSAR data to find crises like land-

slides, rubble flows, etc. Their key plan was to contrast the dispersion of photos and information they received from POLSAR before and after the accident. According to polarimetric evaluation, the general population will stay away from the area where the landslide will occur, and, if needed, individuals will have to be moved. In [40], landslide detection and tracking (LDMWSN) is carried out with the assistance of a hybrid wireless system. One of the best things about this idea is that it uses sender and receiver nodes, which makes it possible to get the best results at the lowest cost. With a portable sensor network, Asian countries can keep an eye on landslides while protecting our way of life. In [41], CAD and CAE are used to keep an eye on landslides, helping them to last six times longer than the CDC scenario. In [42], a landslide tracking mechanism is created using a picture and a geological sensor, and a simulation environment is created to test the usefulness and workability of the component. In [43], WSN is used to look at the chance of a landslide. The suggested approach is very flexible and can operate even when things go wrong. It also has a self-organizing system.

Bu-Chin Wang [44] came up with a way to track landslides using an antenna array and a dual-receiver scheme. The setup records the separate signals in a way that makes sense, and landslide progress can be predicted depending on how the frequency differential varies. A comprehensive demonstration of the 3-D landslide monitoring approach is described. In [45], they suggested a way to find landslides using a VHF blend radar that can be found quickly through contrasting radar images from regular weather and thunderstorm conditions. In this way, steps can be taken to deal with the effects of an emergency. In [45,46], PSI and artificial array radar are used to track landslides and provide a vast amount of information on how the land is changing at a small level. SAR is used in [46] to find shocks caused by landslides. It also starts to keep an eye on places that are likely to be affected early on so that any hazards can be managed.

Landslide detection systems have evolved significantly, incorporating various remote sensing techniques and machine learning algorithms to improve accuracy and reliability. These systems use a variety of data sources, including satellite imagery, LiDAR, and ground-based sensors, to monitor and predict landslide occurrences [47]. Machine learning approaches have shown promising results in landslide detection. A study using remote sensing data and topographic characteristics from the Sikkim region in Malaysia demonstrated that the Support Vector Machine (SVM) algorithm outperformed other algorithms, achieving a precision of 96. 7% and an F1 score of 0.97 [48,49]. The integration of IoT and cloud computing in power systems to enhance efficiency and sustainability. IoT enables seamless communication across the grid, while cloud computing handles data processing and resource management. The merging of IoT and cloud (CoT) drives innovation in energy distribution, renewable energy, and electric vehicle technologies, paving the way for a future of sustainable energy [50,51,68,69]. Table 1 demonstrates different early warning land slide monitoring systems

1.1.2. Research gaps

The following research gaps were identified in the existing body of work related to landslide monitoring systems:

1. High Energy Consumption in Wireless Sensor Networks (WSNs): Most existing landslide monitoring systems exhibit high energy consumption, limiting the operational lifespan of sensor nodes and reducing the overall efficiency of the system.
2. Limited Incorporation of Key Geotechnical Parameters: Many approaches fail to integrate critical parameters such as matric suction and rainfall-induced changes in soil properties, which are essential for accurate landslide prediction.
3. Inefficient Data Routing and Network Performance: Traditional routing methods often result in data latency, packet loss, and reduced throughput, which compromise real-time monitoring and decision-making capabilities.
4. Lack of Scalability and Adaptability: Existing solutions struggle to scale effectively for large and complex terrains, such as regions with varying soil and climatic conditions, and exhibit poor adaptability to environmental changes.
5. Limited Real-World Validation: Many studies focus on simulation-based validation without extensive real-world deployments, leading to uncertainties about their performance under practical conditions.
6. Insufficient Integration of Optimization Techniques: While Particle Swarm Optimization (PSO) and Fuzzy Logic (FL) have been used individually, there is a lack of integration of these methods for comprehensive optimization in landslide monitoring systems.
7. Inadequate Benchmarking Against Modern Approaches: Comparisons with state-of-the-art systems are limited, making it difficult to assess the relative performance of newer techniques.
8. Weak Early-Warning Capabilities: Many systems lack effective early-warning mechanisms to provide timely alerts for disaster mitigation and preparedness.

1.2. Differences between the existing and proposed work

The differences between the investigation that already exists and the work suggested need to be defined with regard to the things that they are attempting to accomplish as well as the key results. Here are some details about these differences:

1. Many other techniques, in contrast to the FLPSO, did not take into account the matric suction that the landslide detection device determined.
2. FLPSO differs from other algorithms because it is designed to measure unsaturated properties for natural slope-stability.
3. The present approaches are not good for many real-time applications because of things like the cost of computing. FLPSO, on the other hand, is said to be the best algorithm for computing.
4. The suggested method is different and more important than others because it takes into account five things that haven't been taken into account before.

1.3. Objectives

The details of our main activities are as follows.

1. Develop an Energy-Efficient Landslide Monitoring System: Design and implement a Wireless Sensor Network (WSN)-based monitoring system using the Fuzzy Logic-based Particle Swarm Optimization (FLPSO) approach to optimize energy consumption and enhance system efficiency.
2. Incorporate Critical Geotechnical Parameters: Integrate key factors such as rainfall, matric suction, and soil stability into the monitoring system to improve the accuracy of landslide prediction.
3. Optimize Data Routing and Task Execution: Utilize FLPSO to create an efficient data routing and task scheduling mechanism that reduces latency, packet loss, and energy consumption while improving throughput and task energy efficiency.
4. Validate System Performance Through Real-World Deployment: Conduct a case study in Shiradi village, Mangalore, a region prone to landslides, to test and validate the system's performance under real-world conditions.
5. Benchmark Against Existing Methods: Compare the proposed system with state-of-the-art techniques such as AEEF [18], LDCSPC [19], LDMWSN [20], and EEELDS [21] to demonstrate improvements in Packet Delivery Ratio (PDR), Energy Delay Product (EDP), Packet Loss Ratio (PLR), task delay, and throughput.
6. Enhance Disaster Preparedness: Develop an early-warning landslide detection mechanism that ensures timely alerts for effective disaster response and mitigation.

Table 1
Comparison of different early warning landslide monitoring system.

Approach	Reliability	Routing	Existence	Size	Early Warning System
[18]	Yes	Multi-Hop	Homogeneous	Even	Yes
[19]	Yes	Multi-Hop	Heterogeneous	Uneven	Yes
[20]	Yes	Multi-Hop	Homogeneous	Uneven	Yes
[21]	Yes	Multi-Hop	Homogeneous	Uneven	Yes
[22]	Yes	Single Hop	Heterogeneous	Uneven	No
[23]	Yes	Single Hop	Heterogeneous	Even	No
[24]	NO	Single Hop	Heterogeneous	Even	No
[25]	NO	Single Hop	Heterogeneous	Uneven	No
[26]	NO	Single Hop	Heterogeneous	Even	No
[27]	NO	Single Hop	Homogeneous	Even	Yes
[28]	NO	Single Hop	Homogeneous	Uneven	No
[29]	NO	Single Hop	Homogeneous	Even	No
[30]	Yes	Multi-Hop	Homogeneous	Uneven	Yes
[31]	Yes	Single Hop	Heterogeneous	Even	No
[32]	NO	Multi-Hop	Heterogeneous	Uneven	Yes
[33]	NO	Multi-Hop	Homogeneous	Even	No
[34]	Yes	Multi-Hop	Heterogeneous	Uneven	Yes
[35]	Yes	Multi-Hop	Heterogeneous	Even	No
[36]	NO	Single Hop	Homogeneous	Even	No
[37]	NO	Single Hop	Homogeneous	Uneven	No
[38]	NO	Single Hop	Heterogeneous	Uneven	Yes
[39]	Yes	Single Hop	Heterogeneous	Even	No
[41]	Yes	Multi-Hop	Homogeneous	Uneven	Yes
[42]	Yes	Multi-Hop	Homogeneous	Uneven	Yes
[43]	Yes	Multi-Hop	Homogeneous	Uneven	Yes
[44]	Yes	Multi-Hop	Homogeneous	Uneven	Yes
[45]	Yes	Multi-Hop	Homogeneous	Uneven	Yes
[46]	Yes	Multi-Hop	Homogeneous	Uneven	Yes
[47]	Yes	Multi-Hop	Heterogeneous	Uneven	Yes
[48]	Yes	Multi-Hop	Heterogeneous	Uneven	Yes
[49]	Yes	Multi-Hop	Heterogeneous	Uneven	Yes
[50]	Yes	Multi-Hop	Heterogeneous	Uneven	Yes
[51]	Yes	Multi-Hop	Heterogeneous	Uneven	Yes

2. Fuzzy logic-based particle swarm optimization MIP in landslide monitoring system

Rainfall often triggers landslides by destabilizing slopes, primarily due to an increase in pore water pressure as groundwater levels rise or as the wetting front infiltrates and saturates the soil. But Fredlund and Rahardjo [52] found that even when it rains a lot, the level of groundwater underneath the surface does not affect the breakdown of weak slopes very much.

In present times, Lu and Godt [53] suggested combining the general idea of optimal load in dry and wet soil circumstances to evaluate the equilibrium of infinite slope failures at shallow depths caused by rain. Fig. 1 shows a cross-section of an essentially infinite slope that assists in clarifying this concept. Here, H_{ss} is the distance from the ground surface to the moving surface, b is the angle of the slope, t is the shear stress, and t_f is the shear strength. Based on the picture, the formula for generic infinite slopes with a factor of safety can be written as eq(1):

$$F_s = \frac{c' + \sigma' \tan \varphi'}{\Gamma H_{ss} \sin \beta \cos \beta} \tag{1}$$

Here, c' is the effective cohesion, φ' is the effective angle of internal friction, and Γ is the unit weight of the sliding mass.

Instead of surges in water level, the progression of the soaking front due to the penetration of rainwater typically causes minor collapses in the context of natural slopes [54,55]. Due to the penetration of precipitation, the unsaturated soil over the groundwater aquifer becomes progressively flooded, leading to a reduction in adverse inlet fluid stress. This leads to a reduction in actual tension as a result of various degrees of suction pressure in the porous humus, which affects the durability of permeable slopes [53–55]. Consequently, several studies are currently monitoring unsaturated characteristics for the natural stability of slopes [55–60]. A common variety of landslides in the Shiradi Ghats, shallow landslides arise at levels of less than 1 m [30]. It is essential to take into account actual stress at various levels [61–65,67–71] due to the occurrence of slope breakdowns as a result of the varying levels of water in slopes that form during rainfall.

2.1. The design architecture of landslide monitoring system

The Landslide Monitoring System (LMS) must be adept at collecting real-time data from multiple sources to obtain up-to-date tracking data. This study recommends a smart sensing system for monitoring unusual sensor data variance that can track any modifications in the characteristics of each tracking sensor over a period of time and execute the gathering, perception, recognition, integration and transfer of the tracking sensors. Through the implementation of a smart gathering technique that uses a sensor anomalous data trigger collection and encoding collection strategy, a landslip catastrophe autonomous system and a dynamic surveillance system suited to complicated field environments are developed.

The slave node is an optimized sensor, data collection device, and battery source design. It emphasizes the collection of information from sensors at every point of observation of the landslide. (1) acquiring information from sensors; and (2) developing agent-based middleware (eagilla) [66] that incorporates mobile agents and transmits information to the parent node. The main purpose of the Master Node is to implement bilateral protocol regulation on a cloud server and capture information about monitoring from each slave node. The sinking device

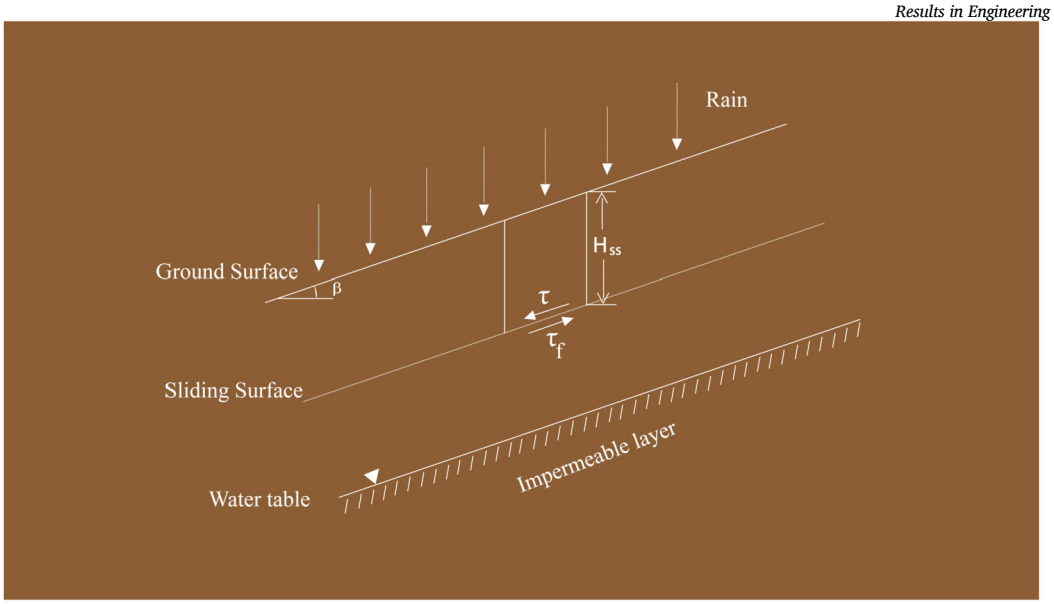

Fig. 1. Cross-sectional diagram of infinite slop-stability analysis.

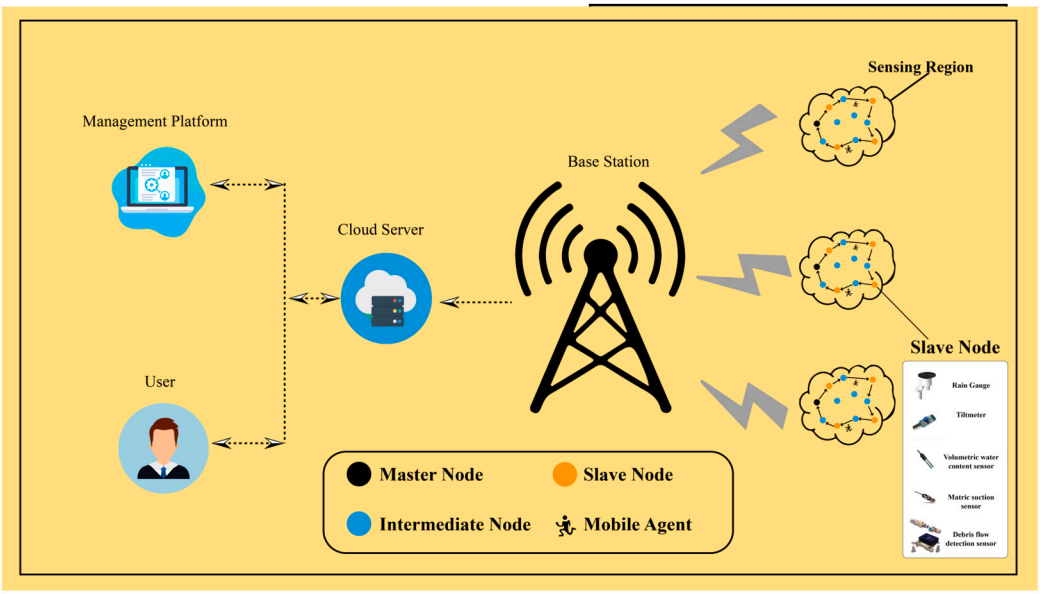

Fig. 2. Architecture of landslide monitoring system.

gathers tracking data from each sub-node and transmits it to the cloud server via 4G. In addition, the master node provides the data collection functionality; the sink node normally handles the rainfall collection job. A cloud server is advantageous because it allows system managers and developers to manage hardware and software with more ease and efficiency. This happens because a cloud server virtually gives processing power to the client, ensuring effective resource utilization. In addition, it enables reliable storage and distribution of tracking information by consolidating disparate sources into a central node, thereby eliminating the requirement for intricate administration by each user. Taking these benefits into account, a cloud server was developed, as depicted in Fig. 2, to ensure reliable system functions while reducing infrastructure setup and maintenance costs. The embedded sensors, data collection loggers, communication devices (LTE modem), an information acquiring system, and a G-cloud server are responsible for transmitting the information gathered from the landslip monitoring stations. Through a web service, clients can gain insight into the server's database.

2.2. FLPSO input parameters

As previously indicated, our proposed FLPSO technique utilizes the three parameters in FLM. In order to prevent the issue of the fuzzy rule eruption, we capped the input variables to three. The sophistication of the rule base in the suggested technique will increase as the number of input variables in FLM increases. But a technique like hierarchical fuzzy systems (HFS) [55], aims to minimize the rule base while preserving appropriate precision.

2.3. Initialization

A wide variety of swarm sensor particles are present in the FLPSO. The sensor particle is indicated P_i. Each sensor particle in physical coordinates, D has different positions [56]. The distinct position of the i^{th} sensor particle P_i is illustrated in Eq. (2).

$$P_i = [P_{i,1}, P_{i,2} \ldots \ldots .. P_{i,D}] \tag{2}$$

Each position of the sensor particle $P_{i,1}$ has the coordinate $(x_{i,1}, y_{i,1})$ in the network space, and its illustration is given in Eq. (3).

$$\mathrm{P_i} = [(\mathrm{x_{i,1}}, \boldsymbol{y_{i,1}}), (\boldsymbol{x_{i,2}}, \boldsymbol{y_{i,2}}) \ldots\ldots (x_{i,D}, y_{i,D})] \tag{3}$$

where i represents the number of sensors.

2.4. Computational parameters

2.4.1. Node's remaining energy

This variable represents the residual energy of a node. All nodes begin with the same amount of initial energy. The initial data collection task initiates and the nodes lose energy due to the MA migration procedure. The calculation is given in Eq. (4).

$$RE\left(P_i\right) = \frac{E_{depleted}}{E_{initial}} \tag{4}$$

2.4.2. Distance to the source node

The variable indicates the proximity between a contender node and SN. Since the sink provides the topographical details of all the network nodes, it is simple to calculate the distance among any intermediate sensors. Given that the rate of MA mobility changes with respect to the path length between sensors, the next hop of the MA should be the potential node with the shortest route from the subsequent SN [57]. To determine the separation between each shortlisted node and the following potential node, use Eq. (5).

$$D(C) = \sqrt{(P_x - C_x) + (P_y - C_y)} \tag{5}$$

where (P_x and P_y) indicates the position of the next SN coordinates, and (C_x and C_y) calculate the position of every potential node.

2.4.3. Number of neighbors

The variable represents the number of nodes within the range of each potential node in the current MA position. The set of potential neighbors is utilized to ensure that MA has an adequate set of SN for successive hop determinations [11], as a result of the multi-hop mobility paradigm used for MA-based information gathering. In some circumstances, if MA approaches a node with fewer neighbors and the residual energy is deficient, MA may choose any of its neighbors as its subsequent hop. Choosing a sensor with little RE will result in discarding the MA as a necessary consequence. Therefore, using the degree of candidate neighbors as one of the FLM's deciding variables can improve efficiency.

2.5. FLM design in PSO

The primary purpose of the research is to determine the best path of MA using PSO. The suggested FLPSO technique computes the MA route for the next hop decision, considering three factors [58]. Fuzzification, rule-evaluation, aggregation, and defuzzification are the foundational elements of the FLM paradigm [59]. FLPSO chooses the conditional probabilities of each potential node as the following MA path and then computes the hop using them. The following describes the four phases of operations in more detail:

2.5.1. Fuzzification

In Fig. 3, the step receives the precise input parameters for every candidate node. The membership function and the lexical parameter are essential in a fuzzy set to properly reflect the actual value in a given circumstance. Instead of numbers, the parameters of a fuzzy set include statements or phrases. The triangular and trapezoidal membership functions in FLPSO are taken into account in this research to analyze the linguistic term in the fuzzy set in Eq. (6) and Eq. (7). Due to their suitability for real-time activities and simple calculations [60], triangular and trapezoidal membership functions are used in this study for fuzzy input and output variables. The triangular membership function is commonly depicted in Eq. (6)

Table 2
Fuzzy IF-THEN rules in FLPSO approach.

Remaining Energy	Distance	Node Neighbor	probability
Low	Far	Small	V-Low
Low	Far	Medium	V-Low
Low	Far	Large	V-Low
Low	Medium	Small	V-Low
Low	Medium	Medium	V-Low
Low	Medium	Large	Low
Low	Close	Small	V-Low
Low	Close	Medium	Low
Low	Close	Large	L-Low
Medium	Far	Small	V-Low
Medium	Far	Medium	Low
Medium	Far	Large	Low
Medium	Medium	Small	V-Medium
Medium	Medium	Medium	Medium
Medium	Medium	Large	L-Medium
Medium	Close	Small	V-Medium
Medium	Close	Medium	Medium
Medium	Close	Large	L-Medium
High	Far	Small	V-Low
High	Far	Medium	Low
High	Far	Large	L-Low
High	Medium	Small	L-High
High	Medium	Medium	High
High	Medium	Large	High
High	Close	Small	V-High
High	Close	Medium	V-High
High	Close	Large	V-High

$$\mu_{C1}(w) = \begin{cases} 0 & w \le d1 \\ \frac{w-d1}{e1-d1} & d1 \le w \le e1 \\ \frac{f1-w}{f1-e1} & e1 \le w \le f1 \\ 0 & f1 \le w \end{cases} \tag{6}$$

$d1$, $e1$ and $f1$ are parameters that determine the shape and position of the triangle. The trapezoidal membership function is commonly depicted in Eq. (7).

$$\mu_{C2}(w) = \begin{cases} 0 & w \le d2 \\ \frac{w-d2}{e2-d2} & e2 \le w \le f2 \\ 1 & e2 \le w \le f2 \\ \frac{f2-w}{f2-e2} & f2 \le w \le g2 \\ 0 & g2 \le w \end{cases} \tag{7}$$

$d2$, $e2$, $f2$ and $d2$ that describe the shape and position of the trapezoidin.

Fig. 4 shows the membership function of residual energy. The Low ranges from 0 to 0.1, the High ranges from 0.9 to 1. Finally, Medium is 0.5.

Fig. 5 shows the membership function of distance. The close ranges are from 0 to 0.5, while the far is 0.6 to 1. The Medium variable is 0.5.

Fig. 6 shows the membership function of the Number of neighbors. Small, Medium, and Large are the output data of the membership function; the attribute set's values are indicated. The small variable is 0 to 0.1 while the High is 0.3 to 1 and the Medium attribute sets to 0.2.

2.5.2. Rule evaluation

The novel fuzzy output group is determined by the IF-THEN rules, which are written as a group of IF-THEN sentences, and the membership values. The fuzzy (AND) function evaluates many inputs to the IF-THEN rules. In this study, three input variables are used, and each variable has three dimensions. IF-THEN rules as shown in Table 2.

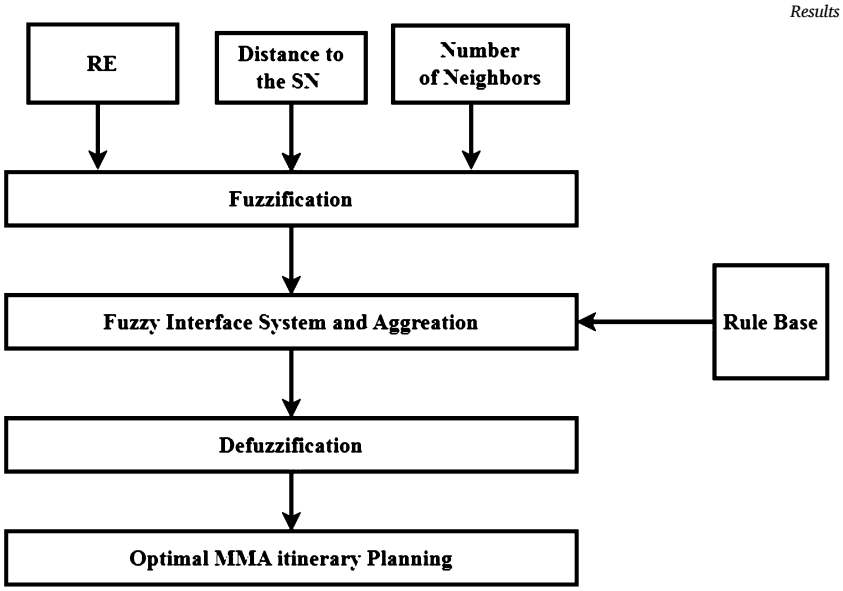

Fig. 3. FLPSO inference system.

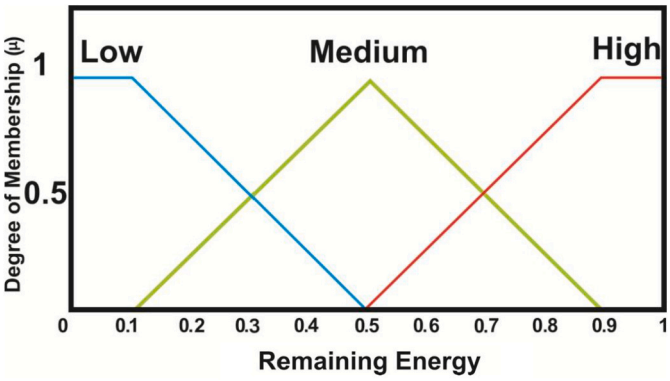

Fig. 4. RE degree of membership function.

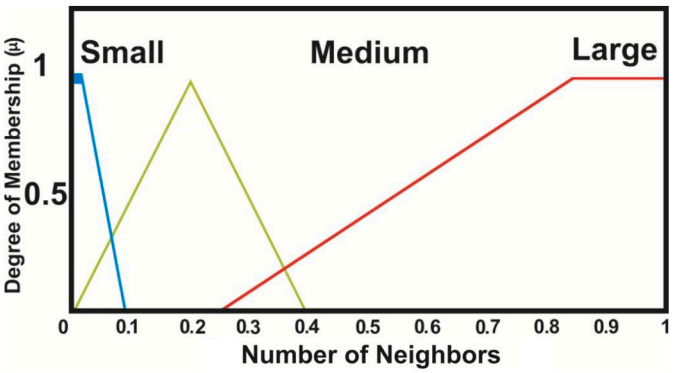

Fig. 6. Node neighbor degree of membership function.

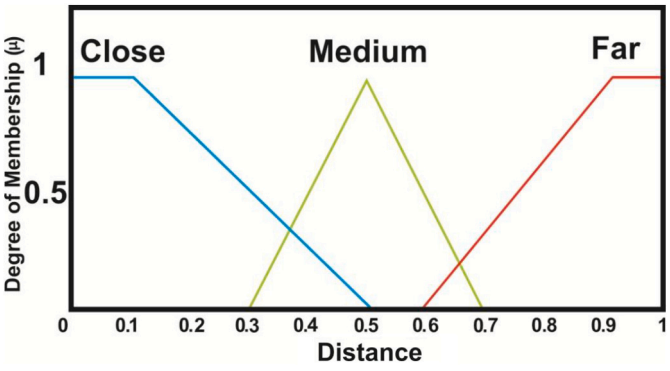

Fig. 5. Distance degree of membership function.

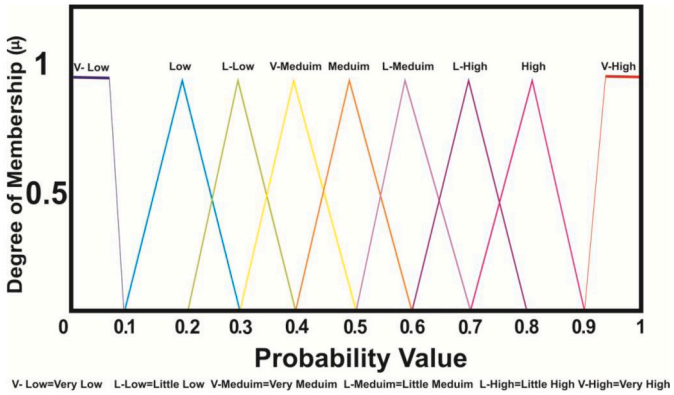

Fig. 7. Membership of the probability value.

2.5.3. *Fuzzy inference system and aggregation*

The observations are made to integrate the rules and obtain a fuzzy output. We employ the Mamdani method [62], the most widely used fuzzy inference methodology, because it is straightforward to determine the output value of every potential node.

2.5.4. *Defuzzification*

After aggregating the outputs for each rule, the defuzzification process is used to produce a crisp result. The crisp final value is obtained using a defuzzification technique called the center of area (CoA) [63], which may be calculated using Eq. (8).

$$CoA(w) = \frac{\int \mu_c(w) w dw}{\int \mu_c(w) dw} \tag{8}$$

In Fig. 7, the linguistic variables of the probability value are divided into nine levels, where w indicates the defuzzifier output and $\mu c(w)$ represents the aggregated membership function.

2.5.5. Velocity and practice position update

During each iteration t, the sensor particles P_i reach their respective positions, specifically P_{best} and G_{best}. Each sensor particle strives to reach G_{best} by updating its velocity $Vel_{i,d}$ and positions P_i in each iteration. Eq. (9) provides the calculation for the velocity $Vel_{i,d}$.

$$Vel_{i,d}(t) = w \times Vel_{i,d}(t-1) + c_1 \times rand_1 \times (P_{Pbest_{i,d}} - P_{i,d}(t-1) + c_2 \times rand_2 \times (P_{Gbest} - P_{i,d}(t-1)) \quad (9)$$

where c_1 *and* c_2 indicate the accelerate factor, such as constant value, w indicates the inertial weight and $rand_1$ *and* $rand_2$ indicate the random values between 0 and 1. The update of P_i is given in Eq. (10).

$$P_{i,d}(t) = P_{i,d}(t-1) + Vel_{i,d}(t-1) \quad (10)$$

2.5.6. Fitness function evaluation

After each iteration, the sensor particles reach the new positions, and the fitness function verifies that the particle reaches the Gbest. The fitness function evaluation formulas are given in the Eq. (11) and Eq. (12).

$$P_{best_i} = \begin{cases} P_i & if \ \left(Fitness\left(P_i\right) < Fitness\left(P_{best_i}\right)\right) \\ P_{best_i} & Otherwise \end{cases} \quad (11)$$

$$G_{best} = \begin{cases} P_i & if \ \left(Fitness\left(P_i\right) < Fitness\left(G_{best}\right)\right) \\ G_{best} & Otherwise \end{cases} \quad (12)$$

2.6. Fuzzy logic-based particle swarm optimization MIP

Our research focuses on detecting rainfall-induced landslides; therefore, the most pertinent information must be acquired during the period of heavy rainfall. Using subsurface stress-based rainwater alert levels of difficulty, we created a limit that influences geological node data collection and the delivery of information to upper layers. In addition to these strategies, state-level shifts are being integrated into the WSN. Both approaches decrease the amount of energy utilized per node, which contributes to a reduction in overall power usage. The novel FLPSO MIP technique method employs FLM to determine the probability of a categorized cluster establishing itself based on their input factors, thereby computing the number of hops that MA must traverse between each pair of slave nodes as shown in Fig. 8. The master needs to maintain an account in a global database regarding all the slave nodes in order to divide the system and ascertain the traveling route of every MA. The next slave node to be visited, before dispatching these individuals out into the system to gather data. While Fuzzy Logic is used to find the sequence of nodes that are intermediary, the PSO approach is used to establish the sequencing of slave nodes. Then, PSO will select the following node for MA and MA's sequence. Once all MA paths for every section have been identified and relocated, the same procedure will be followed for each subsequent journey. The pseudocode of FLPSOMIP for WSN is given in Algorithm 1.

Algorithm 1 FLPSO algorithm.

Inputs:
Initialize routeways of MA A = {a_1, a_2, …, a_m } .
Number of Mobile Agents is k and Size N. r = 0, Number of rounds is r and Maximum Number of rounds r^{max}.
Next_Hop(a_i), ∀i i ≤ 1 ≤ m
Output:
Optimal Route R: → { A+ a_m + 1}
Stepone:
Set number of particles x_i, ∀i i ≤ 1 ≤ N .
Steptwo:
for (i = 1 to N) **do**
  Calculate Fitness(x_i)
  Update P_{besti} , G_{best} .
end for
Stepthree:
while (r < r^{max}) **do**
  for (j = 1 to k) **do**
    for (i = 1 to N) **do**
      Calculate RE(x_i) and DC.
      Determination Fuzzification.
      Apply Rule Evaluation and Aggregation.
      Compute Defuzzification.
      Update Velocity and Practice Position of x_i.
      Determination of Fitness(x_i)
      Update P_{besti} , G_{best} .
    end for
    Stepfour:
    Determine Next_Hop(a_i), ∀i i ≤ 1 ≤ N. (i.e., route R) using G_{best}.
  end for
  r^{max} ++;
end while
Stepfive:

3. Data collection, experimental setup, and geotechnical analysis

This section discusses in further detail the field deployment, Soil Features of the Investigation Area and Analysis of Factor of Safety (FS) using Recorded Data

3.1. Field deployment

The FLPSO tracking devices were deployed to assess variations in stress levels at different levels during precipitation, which could lead to the initiation of small landslides in the native topography. By analyzing both the volumetric water quantity and the suction of the matric, it is possible to determine the actual tension in the unsaturated soil. Consequently, sensors appropriate for gradual slopes in the Shiradi Ghats were chosen on the basis of earlier research and familiarity with unsaturated slope tracking. In addition, a wireless communication-capable gathering device was implemented to facilitate real-time information transfer. In addition to variations in saturation, the volumetric water content and the suction of the matrix have been determined at different levels to determine the fall of the flood front caused by rainfall infiltration. Taking into account that the average level of the soil strata of the natural slope in the Shiradi Ghats is within 2 meters, the nodes were set at levels of 0.5 meters, 1.0 meters and 1.5 meters below the outermost layer of the earth's surface.

The installation of Ubibot RS485 sensors compliant with the international standard ISO enables the monitoring of variations in the volumetric rainwater level in accordance with the center of gravity as precipitation penetrates into the topsoil layers from above. As precipitation percolates into the soil, the moisture front decreases to the soil surface, and saturation occurs as a dampness belt forms. The enlargement of the wetting belt results in the breakdown of the topmost soil layer at shallow levels. MPS-8 sensors were set up to quantify matric suction. The higher layers of soil in natural gradients are unsaturated, and as rainfall penetrates, the shift in moisture conditions causes an alteration in suction stress, which ultimately results in the breakdown of the top soil layer. However, to determine the shift of natural gradients, tilt meters, particularly LM31 sensors, were placed. Additionally, rain gauges have been installed to assess the quantity and severity of precipitation in the region under surveillance. The rain instruments, which utilize the bucket-tipping approach, have been fitted with WTB100 sensors. At the bottom of every surveillance station, an MF4003 sensor was placed to identify and analyze the velocities of the detritus flows. When wires are severed by loads exceeding 150 kgf, a digital signal is generated and communicated to a data recorder.

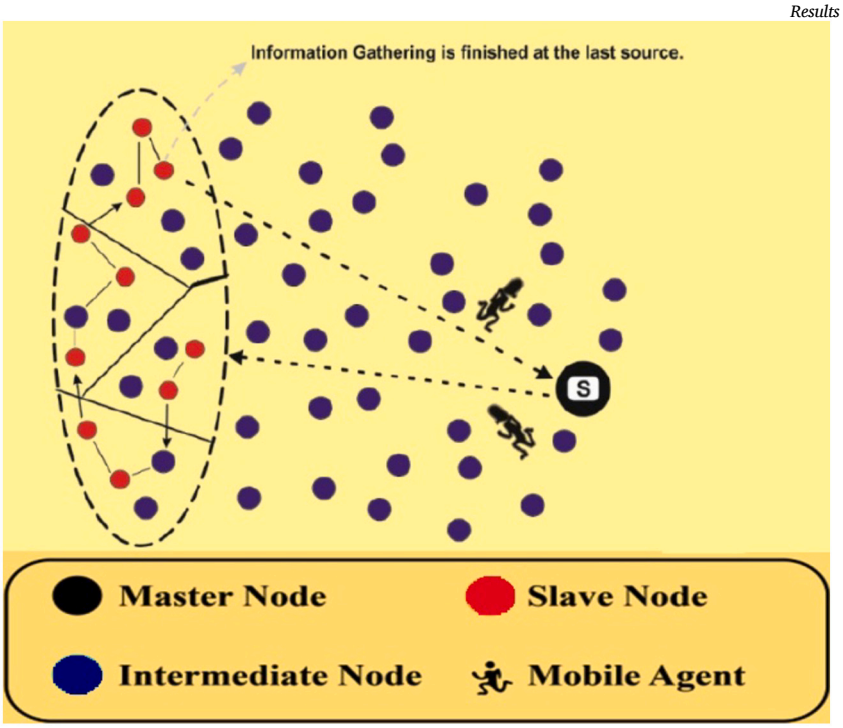

Fig. 8. FLPSO multi-mobile agents itinerary planning in WSN.

Table 3
Samples indicative of the geological properties of the investigated region.

Sl.No	Types	Symbols	Values
1	Distinguished Curve	θ_s θ_r α n m	0.42 0.11 0.31 2.55 0.65
2	Dry Unit Weight	γ_d (kN/m^3)	15.20
3	Effective Cohesion	c' (kPa)	0
4	Angle of Internal Friction	φ' (°)	33.5
5	Percent Fines	(%)	3
6	Liquid Limit	LL (%)	22.8
7	Plastic Limit	PL (%)	-

3.2. Soil features of the investigation area

Field research, selection and numerous soil and characteristic studies were performed to collect information for the slope-stability assessment of the input factors of the evaluation field range. Based on the results of the experiment and the supposition of nearly similar geotechnical characteristics in the area, the data for the input variable necessary to ensure the stability of the slope have been identified, as shown in Table 3. Several investigations [40–42] have established that optimum cohesiveness has little impact on slope-stability gradient involving residual soil and therefore set effective cohesiveness to zero. Furthermore, several international research investigations have proved the efficient cohesiveness of sandy dirt gradients with minimal cohesive impacts at zero [43,44]. Laboratory analysis of five different soil samples acquired within and surrounding the study area revealed that the region is composed of worn sandy soil with a fineness concentration greater than 3%. The actual inside friction angle varied between 29° and 38° in all types of soil.

3.3. Analysis of factor of safety (FS) using recorded data

Landslides in Shiradi occur when excessive rainfall penetrates the soil's level and lowers the tensile force of the substrate beneath a particular level, causing the topsoil to slide down. Such declines in shear force leading to landslides are mainly attributable to an increase in soil saturation and a subsequent reduction in moist pulling stress. Consequently, matric suction, a porous feature of native slope soils, is taken into account in real time to calculate suction tension. In turn, this allows the safety factor to be calculated using an infinite gradient of slope-stability. Fig. 9 shows the variation in rainfall in the factor of safety over a one-year period beginning in 2021 using equation (1). In the formula, the suction levels obtained from the surveillance point matrices and the adaptation factors [38] (Table 3) that correspond to the wet characteristics of the study region were fitted. According to rainfall, the estimated vacuum tension of the soil changed between 0.2 and 2 kPa. As has been stated, once the adhesion tension of the natural slope soil has been determined, the safety factor can be derived. According to the radius of measurement of each sensor, the profundity in the shearing flat surface was assigned to 0.5 m or 1 m in Equation (1). As depicted in the diagram, the difference in F_s was dependent on the difference in soil pressure. At a level of 0.5 m, F_s fluctuated between approximately 1.7 and 1.4, while at a depth of 1 m, the F_s fluctuated between approximately 1.45 and 1.32. Assuming that no landslide incidents occurred and no newly formed landslides were detected during the surveillance period, it appears feasible that F_s was not lowered to < 1.0 during the identical time frame. Consequently, it is feasible to assess factor of safety based on live precipitation following the characteristics of the humus. In addition, the evaluation results emphasize the ability of the tracking system to perform landslip forecasts. By developing landslip prediction limits, which are measures of a slope's instability, alerts can be given based on the calculated F_s in relation to the benchmarks. Significantly, since such early warning techniques utilizing continuous surveillance aren't dependent on forecast information, it will be essential to establish a group of conservative frequency limits to assure sufficient delay.

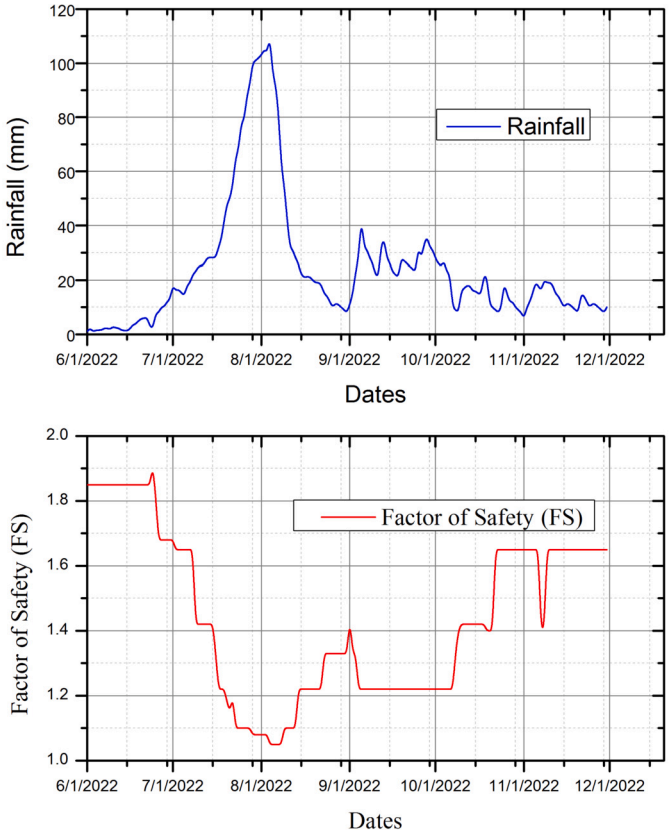

Fig. 9. The impact of rainfall on factor of safety.

4. Simulation, results and discussion

This section discusses in further detail the simulation environment, benchmarks, SOTA approaches used for performance comparison, and statistical analysis.

4.1. Simulation settings

The simulations are performed with MATLAB R2019a. In MATLAB, 100 wireless sensor nodes are set up in a quasi-random manner on a 250 x 120 x 150 m landscape to validate the suggested AEEF [18] clustering algorithm. As previously described, the FLPSO algorithm is initiated at the master node after selecting a suitable route method for transmitting the locations of all slave nodes to the sink node. Now, when a landslide occurs, some sensor nodes will shift and detach independently of the appropriate MA until the overall action stops. The simulation parameters are shown in Table 4.

4.2. Performance metrics

The suggested method's efficiency is validated utilizing typical network matrices such as PDR, EDP, PLR, Task Energy, and Throughput.

4.2.1. PDR

The ratio of data packets accepted by the target node to the number of packets sent by the original node [71].

$$PDR(\%) = \frac{\sum P_r}{\sum P_s} \times 100 \tag{13}$$

where P_r denotes the data packets accepted by the target node. P_s denotes the number of packets sent by the original node.

Table 4
Simulation parameters.

Network Parameters	Value
Size of Network	250 m * 120 m * 150 m
Number of Deployed Nodes	800
Node initial Energy	2 J
Number of Source Nodes	10-100
Transmission Range	60 m
Raw Data Size	2048 bits
MA Processing Code	1024 bits
MA Accessing Delay	10 m
Raw Data Reduction Ratio	0.8
Aggregation Ratio	0.8
Data Processing Time	50 Mbps
Population Size	30
C_1	1.4495
C_2	1.4495
Initial Weight (w)	0.4 to 0.9

4.2.2. EDP

EDP designs for time-sensitive energy applications. Smaller values result in more uniform efficiency.

$$EDP = Energy \times Delay \tag{14}$$

4.2.3. PLR

The ratio of sent packets that are accepted data packets across all delivered packets [71].

$$PLR(\%) = \frac{\sum P_s - \sum P_r}{\sum P_s} \times 100 \tag{15}$$

4.2.4. Task energy

It is the percentage of the overall energy spent by the network's final node by currently available resources [66].

$$Task\ Energy = \frac{\sum N_e}{E} \tag{16}$$

where N_e denotes Energy spent by individual node. E denotes the Total Energy.

4.2.5. Throughput

The mean proportion of correctly collected data packets given the time required throughout the simulation.

$$Throughput = 8 \times S_T \times N_B \times 1000\ Kbps \tag{17}$$

4.3. Performance comparison with the state-of-the-art approaches

The distinctive FLPSO approach is examined compared to SOTA techniques such as AEEF [18], LDCSPC [19], LDMWSN [20] and EEELDS [21]. The methodologies mentioned previously are chosen for the evaluation of FLPSO because of the hybrid nature of the proposed method. When comparing the proposed model approach with the fuzzy and PSO based approaches, it is guaranteed that an accurate analysis will be conducted.

4.4. Results and analysis

The results and analyses are given taking into account the five performance criteria.

4.4.1. PDR

According to Fig. 10, FLPSO performs better than comparable approaches. We alter the scenario's source node range to 100 in order to confirm the efficacy of the proposed method. The FLPSO's consideration of the PDR's master nodes led to the outcomes. Furthermore, FLPSO PDR increases significantly by approximately 14. 15%, 21%, 26.

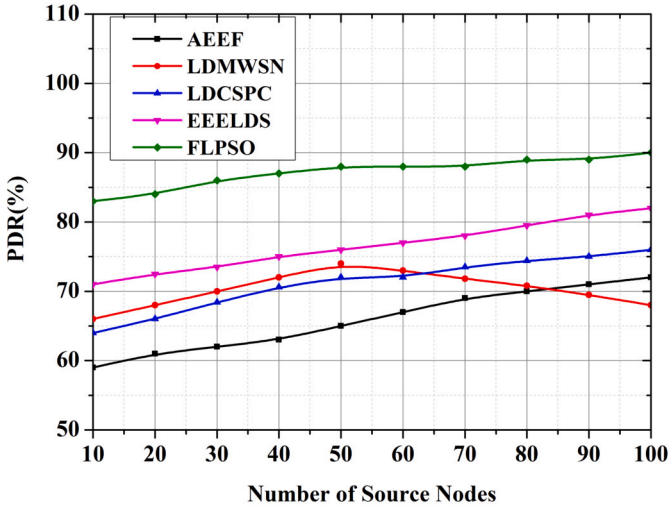

Fig. 10. The impact of number of sensor nodes on PDR.

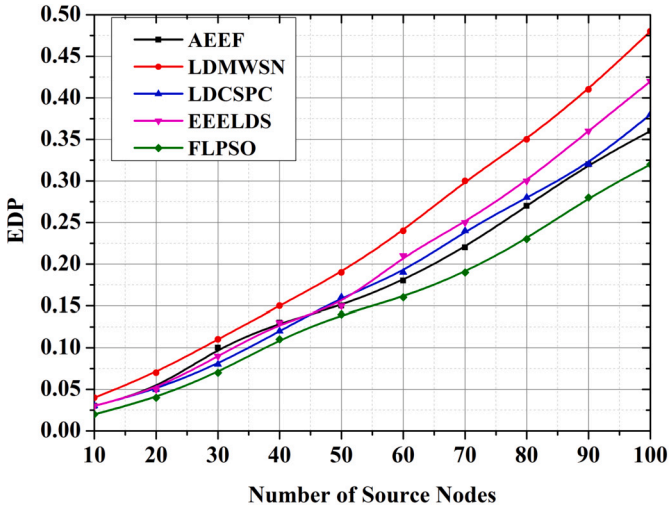

Fig. 11. The impact of number of sensor nodes on EDP.

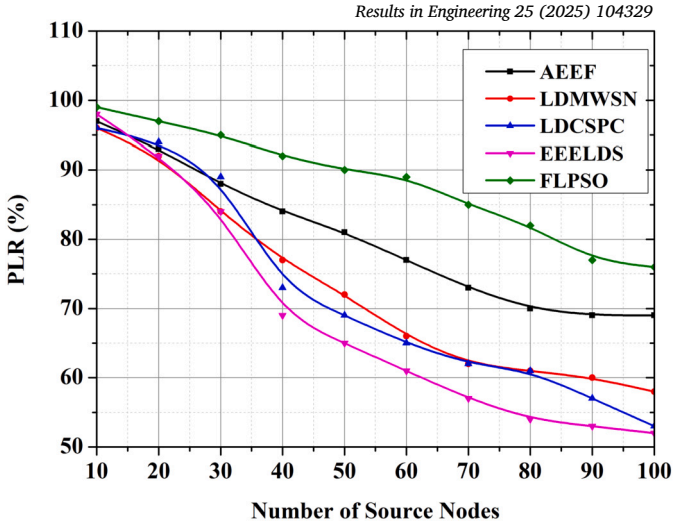

Fig. 12. The impact of number of sensor nodes on PLR.

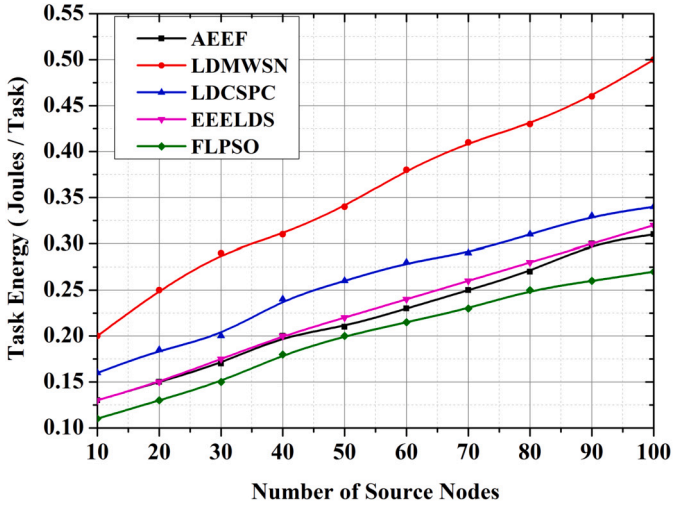

Fig. 13. The impact of number of sensor nodes on Task Energy.

92% and 33% for EEELDS [21], LDMWSN [20], AEEF [18] and LDCSPC [19].

4.4.2. EDP

EDP creates solutions for tasks related to energy and time-critical tasks. The efficacy becomes more consistent when the values are lower. An examination of the total EDP efficiency of the algorithms is shown in Fig. 11. Due to its poorer efficacy in the duration of work over a period of time, leading to the worst execution approach, LDMWSN offers the largest number of energy delay items. FLPSO shortens the task duration more quickly. Furthermore, FLPSO EDP increases significantly by approximately 11. 15%, 15. 12%, 32. 92%, and 43%, respectively, when juxtaposed with AEEF [18], LDCSPC [19], EEELDS [21] and LDMWSN [20].

4.4.3. PLR

As depicted in Fig. 12, FLPSO demonstrates outstanding results compared to competing approaches. We alter the scenario's source node frequency to 100 in order to confirm the efficacy of the proposed method. Because FLPSO took packet transmission into account, the results were obtained. Furthermore, the FLPSO PLR rate increases significantly by approximately 10. 15%, 15. 9%, 25. 26%, and 35. 9% for AEEF [18], LDMWSN [20], LDCSPC [19], and EEELDS [21].

4.4.4. Task energy

The FLPSO technique proposed here uses a smaller amount of energy compared to the AEEF [18], LDCSPC [19], EEELDS[20], and LDMWSN [20] systems. All four approaches require greater effort to complete the task using additional agents. However, compared to other methods, FLPSO is believed to minimize a greater amount of energy. The suggested FLPSO approach achieves energy savings when the sensor frequency range is reduced from 100 to 10, as opposed to 22. 1%, 28. 4%, 33. 57%, and 45. 67% according to AEEF [18], EEELDS [21], LDCSPC [19] and LDMWSN [20], respectively, in Fig. 13.

4.4.5. Throughput

The total amount of data that can be quickly transferred from one SN to a sink node is called throughput. The throughput is significantly improved, as seen in Fig. 14, since packets are transmitted effectively. The throughput of FLPSO significantly increases when contrasted with AEEF [18], EEELDS [21], LDCSPC [19], and LDMWSN [20] by roughly 20.1%, 24.35%, 28.18%, and 35.9%, respectively.

4.5. Statistical analysis

To assess the general relevance of FLPSO, statistical analyzes were conducted. The acquired data are subjected to a Friedman test with a 5% level of confidence. It has been thought to perform a statistical eval-

Table 5
Hypotheses test.

Null hypothesis(H_0)	Alternative hypothesis(H_A)
There is no difference between the dependent variables AEEF [18], LDCSPC [19], LDMWSN [20] , EEELDS [21] and FLPSO	There is a difference between the dependent variables AEEF [18], LDCSPC [19], LDMWSN [20], EEELDS [21] and FLPSO

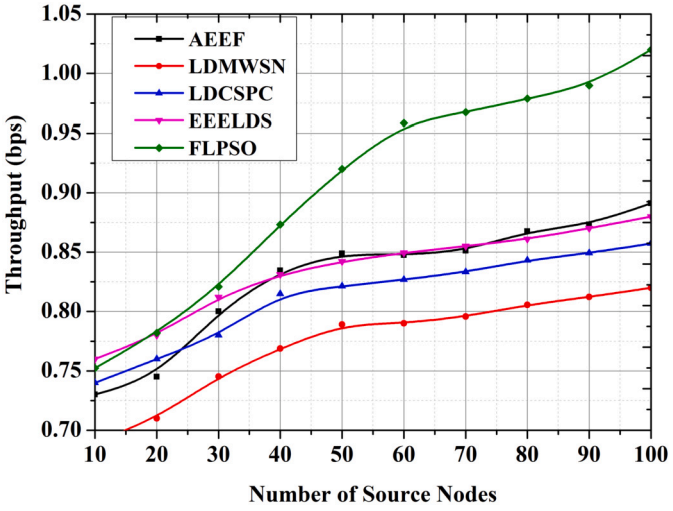

Fig. 14. The impact of source nodes on Throughput.

uation on all parameters. The Null hypothesis (H_0) and the alternative hypothesis (H_A) are shown in Table 5.

This outcome data analysis was obtained using 30 samples that were gathered from all methods. FLPSO beat all other methods, including AEEF [18], LDCSPC [19], LDMWSN [20] and EEELDS [21], according to the results. All parameters were subjected to a Friedman test. The results of the Friedman test indicated that the p-values for all parameters were less than 0.05 (p = 0.000 0.05). Therefore, based on Table 5, H0 is disproved. This finding also shows that one sample is superior to the other. However, it is difficult to determine which algorithms are to blame for the variation in the sample when examining the results. Therefore, pairwise tests are being carried out to assess the outcomes of each member of the group or pair. The FLPSO has shown its abilities noticeably better than the remaining techniques, according to the Table 6. This outcome also shows that the AEEF [18] performed quite well, the EEELDS [21] performed on average, and the LDCSPC [19] and LDMWSN [20] performed the least well.

4.6. Limitations and scope for further work

4.6.1. Limitations

Although the proposed fuzzy logic-based particle swarm optimization (FLPSO) method has shown significant improvements in energy efficiency, task delay, and data reliability for landslide detection systems, certain limitations were observed during the study:

Field-specific parameters The study was carried out in a specific region (Shiradi village, Mangalore, India) with unique geological and climatic characteristics. The results may not be generalized to other regions with vastly different soil properties, rainfall patterns, or topographic characteristics without further adaptation.

Hardware constraints The study relied on specific sensors and wireless network configurations. Variations in hardware capabilities, such as sensor range and battery life, may affect the performance of the system in practical applications.

Computational complexity The FLPSO algorithm incorporates fuzzy logic and optimization techniques, which may lead to increased computational demands in larger networks or real-time systems with limited processing power.

Environmental uncertainty External factors such as extreme weather events, interference in wireless communication, and sensor damage could impact the reliability and robustness of the proposed system.

4.6.2. Scope for further work

Broader field deployments Future studies should test the FLPSO-based system in diverse geographical regions with varying environmental and geological conditions to evaluate its generalizability and adaptability.

Integration with advanced technologies The incorporation of machine learning models and remote sensing technologies, such as satellite imagery and LiDAR, can improve the accuracy of the prediction of landslides and real-time monitoring capabilities.

Energy harvesting solutions Exploring renewable energy sources, such as solar or kinetic energy, to power sensor nodes can reduce the reliance on batteries, extending the operational life of the system.

Resilience to failures Developing fault-tolerant architectures and adaptive algorithms can address issues caused by node failures, communication disruptions, or environmental challenges.

Community integration Future work could focus on integrating the system with community-level early warning platforms to improve public safety and disaster preparedness in vulnerable regions.

5. Conclusion

The Shiradi landslide monitoring system has demonstrated efficacy in assessing rainfall-induced soil behaviors and landslide risks on typical hillside terrains. Through the implementation of long-term surveillance in a slope-prone area of 2 km x 2 km, the study successfully identified key parameters that influence the occurrence of landslides, such as time-dependent changes in soil pressure, slope-stability, and topographical classifications of avalanche danger. The integration of infinite slope-stability calculations, alongside observed matric suction data and deep soil testing, enabled precise computation of safety factors, providing a reliable framework for landslide risk prediction. The ability to correlate precipitation with factor of safety demonstrated the temporal potential of the system in identifying landslide risks with high accuracy.

This study addresses significant limitations in existing landslide detection methods, which often lack prognostic capabilities and rely solely on continuous readings. By incorporating predictive analytics, the proposed system ensures timely detection and notification of potential landslide events, offering a crucial delay for evacuation and mitigation. Furthermore, the design emphasizes the utilization of inexpensive and readily available components, making it a practical and scalable solution for resource-constrained regions. The study highlights the dual merits of precision and efficiency, demonstrating the system's ability to maintain low energy consumption while delivering accurate detection results. Early warning notifications and effective communication of alerts significantly enhance the system's impact, directly contributing to the prevention of disaster-related fatalities. This affordable and

Table 6
Statistics analysis of parameters with respect to algorithms.

Sl.No	Parameters	Algorithms	Ranks	N	Mean	Media	SD	Chi^2	df
1	PDR	AEEF [18]	1.50	30	68.22	69.75	5.34	103.79	4
		LDCSPC [19]	2.53		73.53	74.2	5.04		
		LDMWSN [20]	1.97		68.35	68.4	3.52		
		EEELDS [21]	4		78.47	79.25	4.39		
		FLPSO	5		88.17	89	2.55		
2	EDP	AEEF [18]	2.40	30	0.27	0.26	0.17	106.01	4
		LDCSPC [19]	2.92		0.28	0.27	0.18		
		LDMWSN [20]	5		0.35	0.34	0.22		
		EEELDS [21]	3.68		0.3	0.29	0.2		
		FLPSO	1		0.24	0.22	0.16		
3	PLR	AEEF [18]	3.83	30	76.06	70.5	10.75	104.37	4
		LDCSPC [19]	2.30		65.51	61	16.51		
		LDMWSN [20]	2.58		67.47	61.5	14.3		
		EEELDS [21]	1.32		61.84	54.5	17.14		
		FLPSO	4.97		82.46	82.5	11.31		
4	Task Energy	AEEF [18]	2.42	30	0.3	0.27	0.14	113.54	4
		LDCSPC [19]	4		0.33	0.31	0.14		
		LDMWSN [20]	5		0.45	0.43	0.17		
		EEELDS [21]	2.57		0.29	0.28	0.13		
		FLPSO	1.02		0.27	0.25	0.12		
5	Through-put	AEEF [18]	3.45	30	0.86	0.87	0.06	105.42	4
		LDCSPC [19]	2.15		0.83	0.84	0.05		
		LDMWSN [20]	1		0.79	0.81	0.05		
		EEELDS [21]	3.5		0.86	0.86	0.05		
		FLPSO	4.90		0.96	0.98	0.11		

reliable landslide detection device establishes a benchmark for future innovations in disaster management.

In conclusion, the findings underscore the potential of the Shiradi landslide monitoring system as a transformative approach to landslide risk management. By ensuring early detection, efficient alert transmission, and cost-effective implementation, this model offers a sustainable solution to protect hillside communities and strengthen disaster resilience on a global scale.

6. List of acronyms

The acronyms are shown in Table 7.

Table 7
Nomenclature of FLPSO.

Notations	Definition
MA	Mobile Agent
IP	Itinerary Planning
SIP	Single Mobile Agent Itinerary Planning
MIP	Multi Mobile Agent Itinerary Planning
FLM	Fuzzy Logic model
PSO	Particle Swarm Optimization
SN	Source Nodes
MMA	multi-mobile agents
LMS	Landslide Monitoring System
MEMS	Micro-Electro-Mechanical System
IMU	Inertial Measurement Unit
SIGMA	Sistema Integrato Gestione Monitoraggion Allerta
RSSI	Received Signal Strength Intensity
SHM	Structural Health Monitoring
RSHM	Remote Structural Health Monitoring
PSO	Particle Swarm Optimization

CRediT authorship contribution statement

Lingaraj K: Writing – original draft, Methodology, Investigation, Data curation, Conceptualization. **Rashmi Laxmikant Malghan:** Writing – review & editing, Validation, Supervision, Methodology. **KarthiK Rao M C:** Writing – review & editing, Visualization, Methodology. **Lalit Garg:** Writing – review & editing, Supervision.

Funding

No Funding is available.

Declaration of competing interest

The authors declare that they have no conflict of interest.

Acknowledgements

The authors acknowledge the support from Manipal Institute of Technology, Manipal Academy of Higher Education, Manipal and Rao Bahadur Y. Mahabaleswarappa Engineering College, Bellary for the facilities provided to carry out this research.

Data availability

No data was used for the research described in the article.

References

[1] M. Lee, I. Park, J.-S. Won, S. Lee, Landslide hazard mapping considering rainfall probability in Inje, Korea, Geomat. Nat. Hazards Risk 7 (2016) 424–446.
[2] J.-Y. Park, S.-R. Lee, D.-H. Lee, Y.-T. Kim, J.-S. Lee, A regional-scale landslide early warning methodology applying statistical and physically based approaches in sequence, Eng. Geol. 260 (2019) 105193.
[3] A.M.S. Pradhan, S.-R. Lee, Y.-T. Kim, A shallow slide prediction model combining rainfall threshold warnings and shallow slide susceptibility in Busan, Korea, Landslides 16 (2018) 647–659.
[4] K. Walter, Development of an early warning information infrastructure using spatial web services technology, Int. J. Digit. Earth 3 (2010) 384–394.
[5] E. Nuhn, E. Kropat, W. Reinhardt, S. Pickl, Preparation of complex landslide simulation results with clustering approaches for decision support and early warning, in: Proceedings of the 2012 45th Hawaii International Conference on System Sciences, Maui, HI, USA, 4–7 January 2012, pp. 1089–1096.
[6] D. Graziella, K. Ingeborg, S. Monica, O. Nils-Kristian, E. Ragnar, J. Erik, C. Hervé, Landslide early warning system and web tools for real-time scenarios and for distribution of warning messages in Norway, Eng. Geol. Soc. Territ. 2 (2015) 625–629.

[7] A. Manconi, D. Giordan, Landslide early warning based on failure forecast models: the example of the Mt. de La Saxe rockslide, northern Italy, Nat. Hazards Earth Syst. Sci. 15 (2015) 1639–1644.
[8] G. Acharya, T. Cochrane, T.R.H. Davies, E. Bowman, Quantifying and modeling post-failure sediment yields from laboratory scale soil erosion and shallow landslide experiments with silty loess, Geomorphology 129 (2011) 49–58.
[9] H.R. Pourghasemi, S. Yousefi, A. Kornejady, A. Cerdà, Performance assessment of individual and ensemble data-mining techniques for gully erosion modeling, Sci. Total Environ. 609 (2017) 764–775.
[10] M. Zabihi, H.R. Pourghasemi, A. Motevalli, M.A. Zakeri, Gully erosion modeling using GIS-based data mining techniques in northern Iran: a comparison between boosted regression tree and multivariate adaptive regression spline, in: J.B. Metzler (Ed.), Communicating Climate-Change and Natural Hazard Risk and Cultivating Resilience, Springer, Berlin, Heidelberg, Germany, 2019, pp. 1–26.
[11] Y. Baek, H.B. Koo, K.T. Jang, B.S. Yoo, G.J. Bae, The stability and characteristic analysis of cut slope behavior using real-time monitoring system, J. Eng. Geol. 14 (2004) 71–80 (in Korean with English abstract).
[12] S.D. Cho, K.W. Lee, S.H. Yoon, C.S. Kim, Development of automated slope monitoring system for management and failure forecast of load cut slopes, J. Korean Soc. Civ. Eng. 24 (2004) 1–10 (in Korean with English abstract).
[13] H. Rahardjo, E.C. Leong, R.B. Rezaur, Effect of antecedent rainfall on pore-water pressure distribution characteristics in residual soil slopes under tropical rainfall, Hydrol. Process. 22 (2008) 506–523.
[14] S.J. Harris, R.P. Orense, K. Itoh, Back analysis of rainfall-induced slope failure in Northland Allochthon formation, Landslides 9 (2012) 349–356.
[15] Y.-S. Song, Y.-C. Cho, S. Hong, Analyses on variations in the unsaturated characteristics of a mine waste-dump slope during rainfall, Environ. Earth Sci. (2016) 75.
[16] L. Zhang, B. Shi, D. Zhang, Y. Sun, H.I. Inyang, Kinematics triggers and mechanism of Majiagou landslide based on FBG real-time monitoring, Environ. Earth Sci. 79 (2020) 200.
[17] I.F. Akyildiz, et al., A survey on sensor networks, IEEE Commun. Mag. 40 (2002) 102–114.
[18] S. Ahmed, S. Gupta, A. Suri, S. Sharma, Adaptive energy efficient fuzzy: an adaptive and energy efficient fuzzy clustering algorithm for wireless sensor network-based landslide detection system, IET Netw. 10 (1) (2021) 1–12.
[19] T. Shibayama, Y. Yamaguchi, A landslide detection based on the change of scattering power components between multi-temporal PolSAR data, in: 2014 IEEE Geoscience and Remote Sensing Symposium, 2014, pp. 2734–2737.
[20] G.R. Teja, V.K.R. Harish, D.N.M. Khan, R.B. Krishna, R. Singh, S. Chaudhary, Land slide detection and monitoring system using wireless sensor networks (WSN), in: 2014 IEEE International Advance Computing Conference (IACC), 2014, pp. 149–154.
[21] R. Dhanagopal, B. Muthukumar, A model for low power, high speed and energy efficient early landslide detection system using IoT, Wirel. Pers. Commun. 117 (2021) 2713–2728.
[22] S. Ahmed, S. Gupta, A. Suri, An optimal selection of routing protocol for different sink placements in a wireless sensor network for landslide detection system, in: Proc. of IEEE International Conference on Computational Intelligence and Communication Networks (CICN), Bhopal, India, 2014, pp. 358–363.
[23] G. Barile, G. Ferri, A. Leoni, M. Muttillo, L. Pantoli, V. Stornelli, D. Vettori, Automatic wireless monitoring system for real-time rock fall events, Proceedings 1 (2017) 569.
[24] A. Caviezel, M. Schaffner, L. Cavigelli, P. Niklaus, Y. Buhler, P. Bartelt, M. Magno, L. Benini, Design and evaluation of a low-power sensor device for induced rockfall experiments, IEEE Trans. Instrum. Meas. 67 (2018) 767–779.
[25] P. Giri, K. Ng, W. Phillips, Wireless sensor network system for landslide monitoring and warning, IEEE Trans. Instrum. Meas. 68 (2019) 1210–1220.
[26] D. Vassis, G. Kormentzas, A. Rouskas, I. Maglogiannis, The IEEE 802.11g standard for high data rate WLANs, IEEE Netw. 19 (2005) 21–26.
[27] D. Arosio, L. Longoni, M. Papini, M. Scaioni, L. Zanzi, M. Alba, Towards rockfall forecasting through observing deformations and listening to microseismic emissions, Nat. Hazards Earth Syst. Sci. 9 (2009) 1119–1131.
[28] S.N. Pakzad, G.L. Fenves, S. Kim, D.E. Culler, Design and implementation of scalable wireless sensor network for structural monitoring, J. Infrastruct. Syst. 14 (2008) 89–101.
[29] Crossbow Technology, MicaZ Datasheet, Document Part Number: 6020-0060-04 Rev A, Crossbow Technology, San Jose, CA, USA, 2011.
[30] M.T. Abraham, N. Satyam, B. Pradhan, S. Segoni, A. Alamri, Developing a prototype landslide early warning system for Darjeeling Himalayas using SIGMA model and real-time field monitoring, Geosci. J. 4 (Oct. 2021) 1–13.
[31] L. Benoit, P. Briole, O. Martin, C. Thom, J.P. Malet, P. Ulrich, Monitoring landslide displacements with the Geocube wireless network of low-cost GPS, Eng. Geol. 195 (Oct. 2015) 111–121.
[32] D. Tran, D. Nguyen, S. Tran, Development of a rainfall-triggered landslide system using wireless accelerometer network, Int. J. Adv. Comput. Technol. 7 (5) (2015) 14.
[33] R.F. Romdhane, Y. Lami, D. Genon-Catalot, N. Fourty, A. Lagrèze, D. Jongmans, L. Baillet, Wireless sensors network for landslides prevention, in: Proceedings of the 2017 IEEE International Conference on Computational Intelligence and Virtual Environments for Measurement Systems and Applications (CIVEMSA), Annecy, France, 26–28 June, 2017, pp. 222–227.
[34] C. Wang, W. Guo, K. Yang, X. Wang, Q. Meng, Real-time monitoring system of landslide based on LoRa architecture, Front. Earth Sci. 10 (2022) 899509.
[35] M. Sidorov, P.V. Nhut, Y. Matsumoto, R. Ohmura, LoRa-based precision wireless structural health monitoring system for bolted joints in a smart city environment, IEEE Access 7 (2019) 179235–179251.
[36] P. Mehta, et al. Distributed detection for landslide prediction using wireless sensor network, in: Proceedings of First IEEE Global Information Infrastructure Symposium, Marakech, 2-6 July 2007, pp. 195–198.
[37] K. Georgieva, et al., An autonomous landslide monitoring system based on wireless sensor networks, in: Proceedings of International Conference on Computing in Civil Engineering, Florida, 17–20 June 2012, pp. 145–152.
[38] A. Giorgetti, et al., A robust wireless sensor network for landslide risk analysis: system design, development and field testing, IEEE Sens. J. 16 (6) (2016) 6374–6386.
[39] R. Prabha, et al., Energy efficient data acquisition techniques using context aware sensing for landslide monitoring systems, IEEE Sens. J. 17 (18) (2017) 6006–6018.
[40] R. Prabha, M.V. Ramesh, V.P. Rangan, P.V. Ushakumari, T. Hemalatha, Energy efficient data acquisition techniques using context aware sensing for landslide monitoring systems, IEEE Sens. J. 17 (18) (2017) 6006–6018.
[41] Y. Wang, Z. Liu, D. Wang, Y. Li, J. Yan, Anomaly detection and visual perception for landslide monitoring based on a heterogeneous sensor network, IEEE Sens. J. 17 (13) (2017) 4248–4257.
[42] A. Giorgetti, M. Lucchi, E. Tavelli, M. Barla, G. Gigli, N. Casagli, et al., A robust wireless sensor network for landslide risk analysis: system design, deployment, and field testing, IEEE Sens. J. 16 (16) (2016) 6374–6386.
[43] B.C. Wang, A landslide monitoring technique based on dual-receiver and phase difference measurements, IEEE Geosci. Remote Sens. Lett. 10 (5) (2013) 1209–1213.
[44] Y.Q. Jin, F. Xu, Monitoring and early warning the debris flow and landslides using VHF radar pulse echoes from layering land media, IEEE Geosci. Remote Sens. Lett. 8 (3) (2011) 575–579.
[45] S. Bianchini, F. Cigna, C. Del Ventisette, S. Moretti, N. Casagli, Detecting and monitoring landslide phenomena with TerraSAR-X persistent scatterers data: the Gimigliano case study in Calabria Region (Italy), in: 2012 IEEE International Geoscience and Remote Sensing Symposium, 2012, pp. 982–985.
[46] H. Anandakumar, K. Umamaheswari, Supervised machine learning techniques in cognitive radio networks during cooperative spectrum handovers, Clust. Comput. 20 (2) (2017) 1505–1515.
[47] K. Strząbała, E. Puniach, P. Ćwiąkała, Identification of landslide precursors for early warning of hazards with remote sensing, Remote Sens. 16 (15) (2024) 2781.
[48] M.S. Al-Batah, M. Salem Alzboon, H. Solayman Migdadi, M. Alkhasawneh, M. Alqaraleh, Advanced landslide detection using machine learning and remote sensing data, Data Metadata 3 (2024), https://doi.org/10.56294/dm2024.419.
[49] Q. Liu, Y. Deng, T. Wu, Z. Liu, SE-YOLOv7 landslide detection algorithm based on attention mechanism and improved loss function, Land 12 (8) (2023) 1522, https://doi.org/10.3390/land12081522.
[50] Arul Rajagopalan, Dhivya Swaminathan, Mohit Bajaj, Issam Damaj, Rajkumar Singh Rathore, Arvind R. Singh, Vojtech Blazek, Lukas Prokop, Empowering power distribution: unleashing the synergy of IoT and cloud computing for sustainable and efficient energy systems, Results Eng. (ISSN 2590-1230) 21 (2024) 101949, https://doi.org/10.1016/j.rineng.2024.101949.
[51] Lavanya Kandasamy, Anand Mahendran, Sai Harsha Varma Sangaraju, Preksha Mathur, Soham Vijaykumar Faldu, Manuel Mazzara, Enhanced remote sensing and deep learning aided water quality detection in the Ganges River, India supporting monitoring of aquatic environments, Results Eng. (ISSN 2590-1230) 25 (2025) 103604, https://doi.org/10.1016/j.rineng.2024.103604.
[52] D.G. Fredlund, H. Rahardjo, Soil Mechanics for Unsaturated Soils, Wiley, New York, NY, USA, 1993.
[53] N. Lu, J. Godt, Infinite slope stability under steady unsaturated seepage conditions, Water Resour. Res. 44 (2008) 11404.
[54] Y.-S. Song, W.-P. Hong, K.-S. Woo, Behavior and analysis of stabilizing piles installed in a cut slope during heavy rainfall, Eng. Geol. (2012) 129–130, pp. 56–67.
[55] C. Ng, Q. Shi, A numerical investigation of the stability of unsaturated soil slopes subjected to transient seepage, Comput. Geotech. 22 (1998) 1–28.
[56] L. Comegna, E. Damiano, R. Greco, A. Guida, L. Olivares, L. Picarelli, Field hydrological monitoring of a sloping shallow pyroclastic deposit, Can. Geotech. J. 53 (2016) 1125–1137.
[57] E. Damiano, L. Olivares, L. Picarelli, Steep-slope monitoring in unsaturated pyroclastic soils, Eng. Geol. (2012) 137–138, pp. 1–12.
[58] J.W. Godt, R.L. Baum, N. Lu, Landsliding in partially saturated materials, Geophys. Res. Lett. 36 (2009) 02403.
[59] Y.-S. Song, B.-G. Chae, J. Lee, A method for evaluating the stability of an unsaturated slope in natural terrain during rainfall, Eng. Geol. 210 (2016) 84–92.
[60] J.B. Smith, J.W. Godt, R.L. Baum, J.A. Coe, W.J. Burns, M.M. Morse, B. Sener-Kaya, M. Kaya, Hydrologic Monitoring of a Landslide-Prone Hillslope in the Elliott State Forest, Southern Coast Range, Oregon, 2009–2012, US Geological Survey, Lakewood, CO, USA, 2014.
[61] K.-S. Kim, Y.-S. Song, Geometrical and geotechnical characteristics of landslides in Korea under various geological conditions, J. Mt. Sci. 12 (2015) 1267–1280.
[62] C.M. Wolle, W. Hachich, Rain-induced landslides in Southeastern Brazil, in: Proceedings of the 12th International Conference on Soil Mechanics and Foundation Engineering, Rio de Janeiro, Brazil, 13–18 August 1989, pp. 1639–1644.
[63] T.M.P. de Campos, M.H.N. Andrade, E.A. Vargas, Jr., Unsaturated colluvium over rock slide in a forested site in Rio de Janeiro, Brazil, in: Proceedings of the 6th

International Symposium on Landslides, Christchurch, New Zealand, 10–14 February 1991, vol. 2, pp. 1357–1364.

[64] J.W. Godt, R.L. Baum, A.F. Chleborad, Rainfall characteristics for shallow landsliding in Seattle, Washington, USA, Earth Surf. Process. Landf. 31 (2006) 97–110.

[65] N. Lu, A. Wayllace, S. Oh, Infiltration-induced seasonally reactivated instability of a highway embankment near the Eisenhower Tunnel, Colorado, USA, Eng. Geol. 162 (2013) 22–32.

[66] K. Lingaraj, R.V. Biradar, V. Patil, Eagilla: an enhanced mobile agent middleware for wireless sensor networks, Alex. Eng. J. 57 (3) (2018) 1197–1204.

[67] K.K. Zur, S.A. Faghidian, Nanomechanics of Structures and Materials: Modeling and Analysis, Elsevier Science, 2024, ISBN: 9780443219498.

[68] Toshiki Hatanaka Watanabe, Nakano Shintaro, Valentin Ken Popov, Sliding Friction in Contacts with One- and Two-Dimensional Viscoelastic Foundations and Viscoelastic Half-Space, Facta Universitatis Series Mechanical Engineering, vol. 22, 2024, pp. 529–545.

[69] S.A. Faghidian, I. Elishakoff, Wave propagation in Timoshenko–Ehrenfest nanobeam: a mixture unified gradient theory, J. Vib. Acoust. 144 (6) (December 2022) 061005, https://doi.org/10.1115/1.4055805.

[70] S.A. Faghidian, I. Elishakoff, The tale of shear coefficients in Timoshenko–Ehrenfest beam theory: 130 years of progress, Meccanica 58 (2023) 97–108, https://doi.org/10.1007/s11012-022-01618-1.

[71] S. Karthik, M. Karthick, N. Karthikeyan, S. Kannan, A multi-mobile agent and optimal itinerary planning-based data aggregation in wireless sensor networks, Comput. Commun. (ISSN 0140-3664) 184 (2022) 24–35, https://doi.org/10.1016/j.comcom.2021.11.019.